

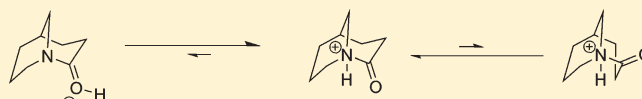
1-Azabicyclo[3.3.1]nonan-2-one: Nitrogen Versus Oxygen Protonation

Brian Sliter, Jessica Morgan, and Arthur Greenberg*

Department of Chemistry, University of New Hampshire, Durham, New Hampshire 03824, United States

Supporting Information

ABSTRACT: Protonation of typical unstrained amides and lactams is heavily favored at oxygen. In contrast, protonation of the highly distorted lactam 1-azabicyclo[2.2.2]octan-2-one is heavily favored at nitrogen. What structures occupy “crossover boundaries” where N- and O-protonation are nearly equienergetic? Density function theory calculations at the B3LYP/6-31G* level, as well as QCISD(T)/6-31G* calculations, predict that 1-azabicyclo[3.3.1]nonan-2-one favors N-protonation at nitrogen only very slightly (<2.0 kcal/mol; “gas phase”) over O-protonation. ¹H and ¹³C NMR as well as ultraviolet (UV) studies of this lactam, in its combination with sulfuric acid, confirm predominant protonation at nitrogen. Although the calculations very slightly favor the N-protonated chair–chair conformation, experimental spectra clearly support the N-protonated boat-chair. Broadened resonances in the ¹³C NMR spectrum suggest an exchange phenomenon. Variable-temperature studies of the ¹³C NMR spectra support dynamic exchange between the major tautomer (N-protonated) and the minor tautomer (O-protonated) in a roughly 4:1 mixture. The findings also support the published prediction that a twisted bridgehead lactam with the nitrogen lone pair (n_N) as HOMO will protonate at nitrogen.



INTRODUCTION

Distortion of the amide linkage, through twisting about the N–CO bond and/or pyramidalization at nitrogen,¹ can significantly modify its chemistry.² Examples include facile thermolysis, as well as hydrolysis under neutral aqueous conditions, of derivatives of “2-quinuclidone” (1-azabicyclo[2.2.2]octan-2-one),^{3–5} and protonation as well as alkylation on nitrogen instead of oxygen.^{3–7} A delicate shift in the balance of structural factors dictates O-protonation (and methylation) of 1-azabicyclo[3.3.2]decan-2-one and N-protonation (and methylation) of its lower homologue 1-azabicyclo[3.2.2]nonan-2-one.⁸ The strain and unique structure of 3,5,7-trimethyl-1-azaadamantan-2-one have provided a fascinating picture of the four-coordinate intermediate in amide hydrolysis.^{9,10} The enhanced reactivities and altered chemistries¹¹ of distorted amide linkages have consequences for the activities of β -lactam antibiotics,¹² mechanisms of proteolytic enzymes,¹³ *cis-trans*-peptidylprolyl isomerases and protein folding,¹⁴ and autocatalytic proteolysis.¹⁵ The discovery of “crossover” geometries in which N- and O-protonation are nearly equienergetic may provide insights into these important issues.

Ab initio molecular orbital calculations (isolated molecule or “gas phase”)⁶ indicate that O-protonation is strongly favored over N-protonation of unstrained amides and lactams and this is consistent with experiment.¹⁶ For example, O-protonated *N*-methyl-2-pyrrolidone (**1**, Scheme 1) is calculated, at the 6-31G* level, with correction for zero-point energy (ZPE) and thermal energy, to be about 15 kcal/mol more stable than the N-protonated tautomer in the gas phase.^{6b} In contrast, N-protonation of 1-azabicyclo[2.2.2]octan-2-one (see **2**) is predicted to be favored by about 23 kcal/mol.^{6b} Closer to the “borderline” (as noted above), **3** is favored over its O-protonated tautomer by 9 kcal/mol while **4** is

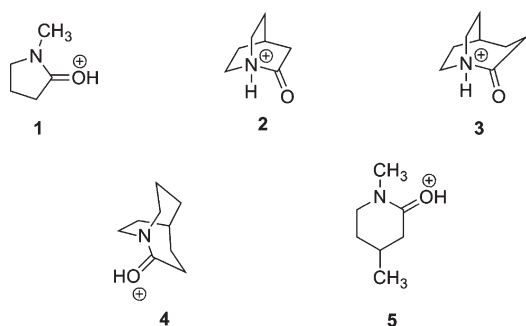
favored over its N-protonated tautomer by about 7 kcal/mol.^{6b} Aqueous solvation, calculated by using the polarizable continuum model (PCM), only slightly modifies these energy differences in the direction favoring the N-protonated tautomer.¹⁷ The calculated free energy differences [$\Delta G_{\text{N-Prot.}} - \Delta G_{\text{O-Prot.}}$ (B3PW91/6-31+G*)] (a) favor N-protonated 1-azabicyclo[2.2.2]octan-2-one (**2**) [–19.7 kcal/mol (gas phase); –21.0 kcal/mol (aqueous)], (b) favor N-protonated 1-azabicyclo[3.2.2]nonan-2-one (**3**) [–4.8 kcal/mol (gas phase); –5.9 kcal/mol (aqueous)], and (c) favor O-protonated *N*-methyl-4-methyl-2-piperidone (**5**) [+16.2 kcal/mol (gas phase); +14.0 kcal/mol (aqueous)].¹⁷

Protonated lactams **3** and **4** are thus calculated, and experimentally inferred,^{4a,d} to be unambiguously N-protonated and O-protonated, respectively. In contrast, N-protonated 1-azabicyclo[3.3.1]nonan-2-one (**6**, Scheme 2) has been calculated to be only 1.4 kcal/mol lower in corrected total energy than the O-protonated tautomer **7**.^{6b} This is close to the “noise level” of such calculations and therefore worthy of experimental investigation. Although, as noted above, aqueous solvation may add an additional 1–2 kcal/mol to the relative stability of **6**, N-protonation (**6**) and O-protonation (**7**) remain quite close in energy. The calculated Dunitz–Winkler amide distortion parameters^{1a} in the preferred boat-chair conformation of the neutral [3.3.1] lactam (**8_{BC}**, see Scheme 3) are as follows: τ (19.8°); χ_{N} (49.7°); χ_{C} (7.2°). The corresponding parameters in an undistorted lactam are as follows: $\tau = \chi_{\text{N}} = \chi_{\text{CO}} = 0^\circ$. An additional comparison is furnished by the sum of the three calculated C–N–C angles: 340.5° in the [3.3.1] lactam versus 360° for planar nitrogen and ca.

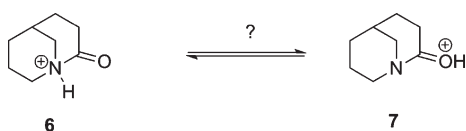
Received: January 26, 2011

Published: March 10, 2011

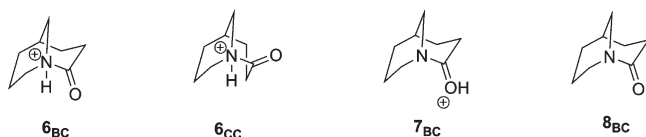
Scheme 1



Scheme 2



Scheme 3



328.5° for an idealized tetrahedral nitrogen. In addition to establishing the favored protonation site, experimental investigation of the [3.3.1] system should also provide a challenging test of the prediction by Werstuijk et al.⁸ that, in twisted bridgehead lactams, those in which the highest occupied molecular orbital (HOMO) corresponds to the nitrogen lone pair (n_N) protonate at nitrogen (e.g., 3), while those in which n_O is the HOMO protonate at oxygen (e.g., 4).

In the present study, 1-azabicyclo[3.3.1]nonan-2-one is dissolved in strong acidic media and the protonated lactam is studied in solution, using ^1H and ^{13}C NMR as well as UV spectroscopy. The experimental results are compared with computational predictions of total energies, free energies, molecular orbital energies, and spectra in order to assign the site of protonation (N vs O) as well as the conformation(s) of the protonated tautomer(s).

COMPUTATIONAL METHODS

Calculations were performed with the Spartan 08¹⁸ as well as the Gaussian 03¹⁹ suite of programs. A Monte Carlo search algorithm was initially performed on the N-protonated and O-protonated conjugate acids of 1-azabicyclo[3.3.1]nonan-2-one at the AM1 level of theory. The geometry of each conformer was optimized at the B3LYP/6-31G* level of theory and single-point energy determinations were performed for the two lowest-energy N-protonated conformers (boat-chair and chair-chair) and the lowest-energy O-protonated conformer (boat-chair) at the QCISD(T)/6-31G* level of theory with GAUSSIAN 03. The transition state between the boat-chair and chair-chair was located by using Spartan 08 at the B3LYP/6-31G* level of theory. It was confirmed as a transition state by having only one imaginary vibrational mode and by IRC in Gaussian 03. The imaginary frequency corresponded to

Table 1. Relative Uncorrected Total Energies (ΔE_T), Relative Total Energies Including ZPE and Thermal Corrections ($\Delta E_T[\text{Corr}]$), Relative Free Energies ($\Delta\Delta G$) for Optimized B3LYP/6-31G* Structures (gas phase), and Relative Total Energies for Solvent Continuum (aqueous) B3LYP/6-31G* Structures, As Well As Relative Energies (ΔE_T) for Single Point QCISD(T)/6-31G* Calculations (all values are in kcal/mol)

protonated structure	B3LYP/6-31G*				QCISD(T)/6-31G*
	ΔE_T	$\Delta E_T[\text{Corr}]$	$\Delta\Delta G$	$\Delta E_T(\text{aq})$	ΔE_T
6 _{CC}	0.00	0.00	0.00	0.00	0.00
6 _{BC}	+0.28	+0.36	+0.71	+0.13	+0.13
7 _{BC}	+0.40	+0.43	+1.38	+5.03	+2.98

movement of the flagpole hydrogen on C3 of the boat-chair toward the equatorial position of the chair-chair. These molecules were also optimized at the B3LYP/6-31G* level by using the solvent polarization continuum model (SM8) in water. The lowest-energy conformer of the neutral lactam (boat-chair) was optimized at the B3LYP/6-31G* level of theory. Calculations of ^1H and ^{13}C NMR spectra were performed with Spartan 08 at the B3LYP/6-31G* level of theory for the lactam and its protonated tautomers.

The two low-energy N-protonated conformers (both pairs of enantiomers) of 1-azabicyclo[3.3.1]nonan-2-one were initiated as hydrogen-bonded dimers at the AM1 level. However, due to Coulombic repulsion in the “gas phase” calculation these dimers separated during optimization. Reasoning that solvation in water would mitigate this repulsion very significantly, the dimer was optimized at the HF/3-21G level of theory by using the continuum model (SM8) in water. Single-point energy calculations were performed upon these structures at the B3LYP/6-31G* level of theory. For purposes of comparison, the two N-protonated and single O-protonated conformers of the monomer were optimized at the HF/3-21G level of theory and single-point energy calculations were performed at B3LYP/6-31G* by using SM8 solvation in water. A similar study was done for the dimer of N-protonated 1-azabicyclo[2.2.2]octan-2-one (“2-quinuclidonium”), which was fully optimized at B3LYP/6-31G* by using SM8 solvation in water.

RESULTS AND DISCUSSION

Scheme 3 shows the calculated lowest-energy conformations for 1-azabicyclo[3.3.1]nonan-2-one (8_{BC}), its O-protonated conjugate acid (7_{BC}), and the two low-energy conformers for the N-protonated tautomer (6_{BC} and 6_{CC}), where “B” and “C” designated boat and chair conformations, respectively. Table 1 lists calculated relative total energies, relative total energies including unscaled ZPE and thermal corrections, relative total energies in aqueous solution, and relative free energies at the B3LYP/6-31G* optimized level for the three protonated species 6_{BC}, 6_{CC}, and 7_{BC}. Additionally, a single-point calculation was made for each of these three structures at the QCISD(T)/6-31G* level by using the DFT-optimized geometries. These calculations support the earlier predictions that N-protonation is favored over O-protonation.⁶ They also very slightly favor 6_{CC} over 6_{BC}. The N–CO bond in 8_{BC} is calculated to be lengthened relative to that in the unstrained lactams *N*-methyl-2-pyrrolidone (1.398 Å vs 1.374 Å) while the C=O bond is calculated to show little variation (1.222 Å vs 1.221 Å). Upon O-protonation, the

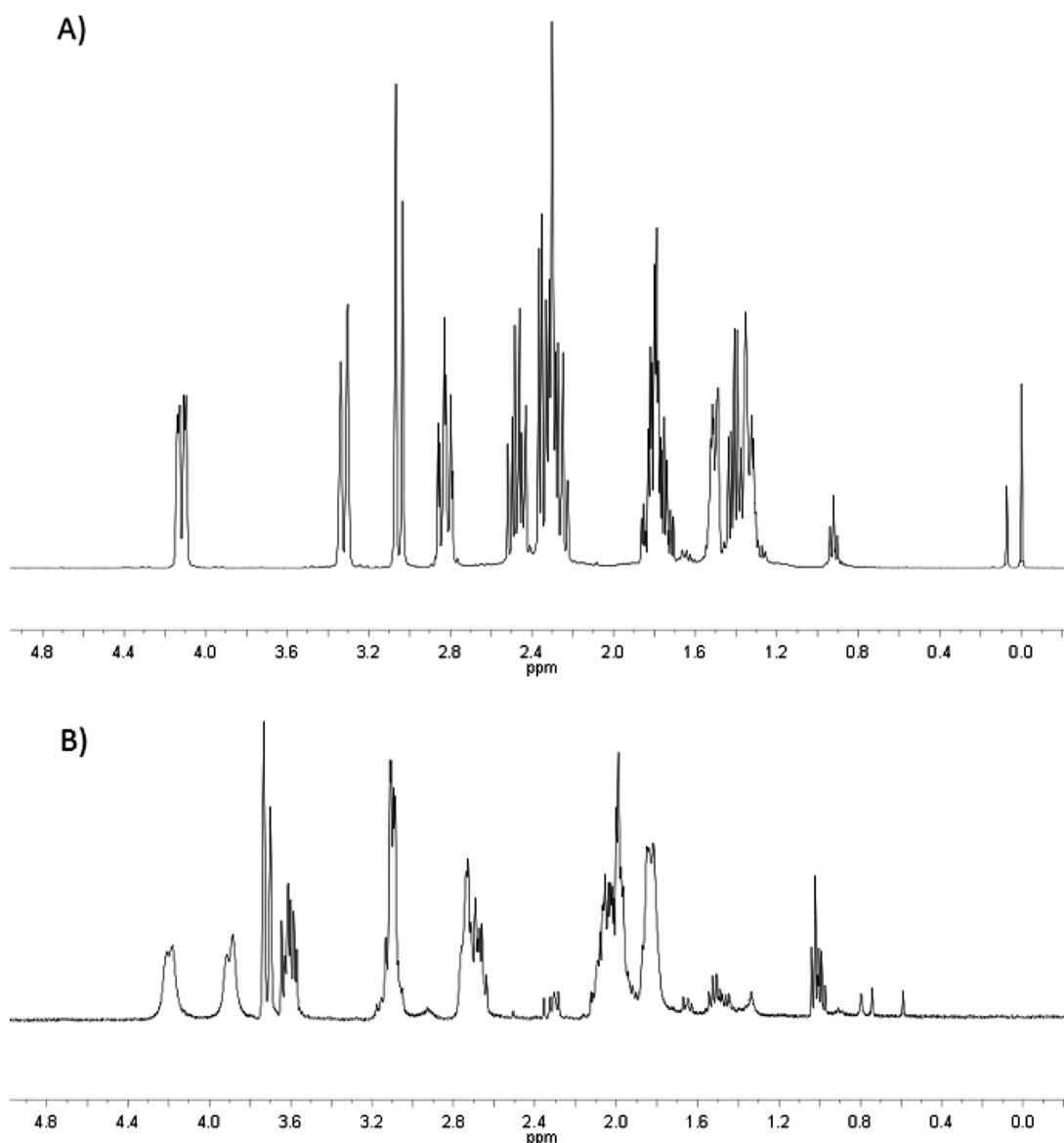


Figure 1. (A) ^1H NMR spectrum (400 Hz) of 1-azabicyclo[3.3.1]nonan-2-one in CDCl_3 ; (B) ^1H NMR spectrum of 1-azabicyclo[3.3.1]nonan-2-one approximately equimolar with H_2SO_4 in deuterated trifluoroacetic acid (TFA-d) solution.

$\text{N}=\text{CO}$ bond in 7_{BC} is predicted to shorten to 1.312 Å and the $\text{C}=\text{O}$ bond lengthen to 1.317 Å. Protonation at nitrogen (e.g. for 6_{BC}) is calculated to lengthen $\text{N}=\text{CO}$ (1.581 Å) and shorten $\text{C}=\text{O}$ (1.187 Å). This is consistent with earlier MP2/6-31G* studies.^{6b}

The ^1H and ^{13}C NMR spectra of 1-azabicyclo[3.3.1]nonan-2-one (8_{BC} in Scheme 3) are displayed in Figures 1A and 2A. Previous analyses²⁰ of the ^1H NMR of this compound provided limited chemical shift assignments due to the complexity of some of the upfield peaks. Computed and experimental assignments for 8_{BC} are listed in Table 2. Buchanan^{20d} analyzed the long-range, W-type coupling of 9H_{eq} (termed 9H_{fp} in the present paper; “fp” = flagpole) with 8H_{eq} as well as 6H_{eq} in 5-phenyl-1-azabicyclo[3.3.1]nonan-2-one, the absence of such coupling between 9H_{ax} and a C-4 proton, and assigned the boat-chair conformation. This was subsequently supported by an X-ray crystallographic study.^{20e} This is consistent with the widely accepted amide-alkene analogy:^{1,2} The boat-chair in this molecule mimics *trans*-cyclooctene

whereas the chair-chair mimics the much more strained *trans*-cyclohexene. The ^1H NMR peak assignments for 8_{BC} in Table 2 were aided by NOESY spectroscopic studies (see the Supporting Information, S.2.13 and S.2.14). Of particular note is the NOESY interaction between 9H_{fp} and 3H_{fp} (calculated distance, 2.177 Å), verifying the boat-chair conformation.

The initial experiment involved dissolving 8_{BC} in pure deuterated trifluoroacetic acid (TFA-d , $\text{pK}_a = 0.52$).^{2f} While this acid should not protonate an unstrained lactam [e.g., $\text{pK}_a(1) = -0.75$],²² it might be capable of protonating this twisted lactam, which has an appreciably pyramidal nitrogen. A previous computational study predicted that the gas-phase proton affinity (PA) of 1-azabicyclo[3.3.1]nonan-2-one is slightly higher than that of *N*-methyl-2-pyrrolidone [difference = 0.9 (6-31G*), 0.5 kcal/mol (6-31G*, with unscaled thermal and ZPE corrections)].^{6b} The B3LYP/6-31G* calculations (including unscaled thermal and ZPE corrections) in the present study predict a gas-phase PA of 218.3 kcal/mol for *N*-methyl-2-pyrrolidone (experimental: 220.7

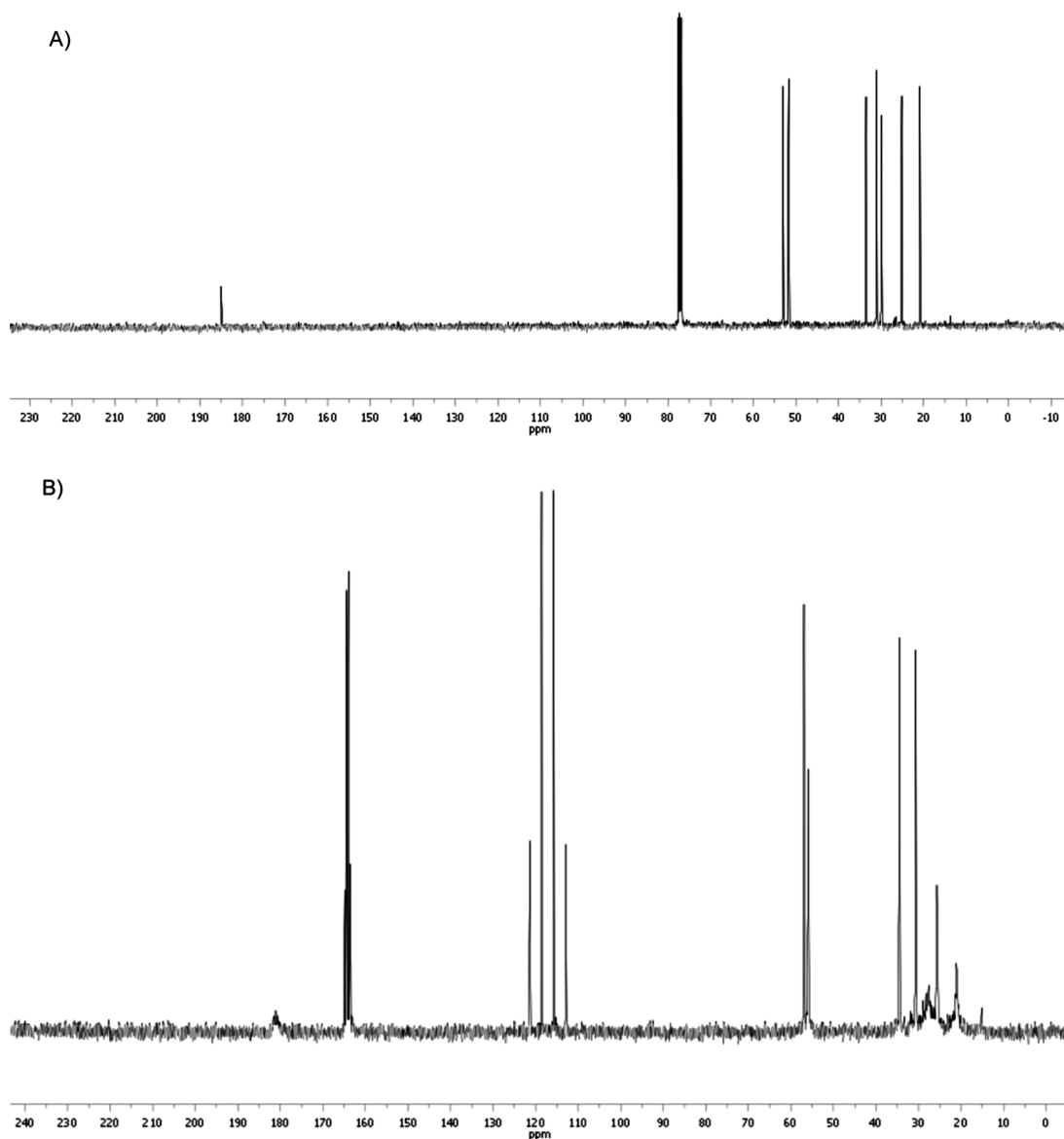


Figure 2. (A) ¹³C NMR spectrum (100 MHz) of 1-azabicyclo[3.3.1]nonan-2-one in CDCl₃; (B) ¹³C NMR spectrum of 1-azabicyclo[3.3.1]nonan-2-one in concentrated H₂SO₄ with added TFA-*d* [see Figure 3A for the corresponding ¹³C NMR spectrum (125 MHz) in approximately equimolar lactam and H₂SO₄ in TFA-*d* solution].

kcal/mol²³). The corresponding DFT calculated value to produce **6_{CC}** is 220.2 kcal/mol, and 219.8 kcal/mol to produce **6_{BC}**. Thus, it was reasonable to investigate whether **8_{BC}** could be protonated in TFA. There was no significant change in the ¹H and the ¹³C NMR spectra in comparing CDCl₃ and TFA-*d* solutions (see the Supporting Information, S.2.4–S.2.6). Hence TFA does not protonate 1-azabicyclo[3.3.1]nonan-2-one. Initial ¹H NMR experiments with mineral acid employed D₂SO₄ and solvent with added TFA-*d* as the internal standard, due to the insolubility of TMS. The two ¹³C quartets of TFA (centered at 116.6 and 164.2 ppm)²⁴ occur in spectroscopic “windows”, and the difference in chemical shifts (47.6 ppm) between the two carbons in TFA remains essentially constant in the solvent system employed (e.g., 47.1 ppm in trifluoroacetic acid with added sulfuric acid, see below). The chemical shift of the hydrogen in TFA (11.5 ppm) served as a useful marker for ¹H NMR. Subsequent experiments employed TFA-*d* as the solvent with roughly equimolar amounts

of **8_{BC}** and D₂SO₄ (or H₂SO₄) as solutes. These acids were usually dry enough not to induce significant hydrolysis of the lactams to its protonated ring-opened amino acid.

Figure 1B shows the ¹H NMR spectrum of approximately equimolar 1-azabicyclo[3.3.1]nonan-2-one and H₂SO₄ dissolved in TFA-*d* (the corresponding ¹³C NMR spectrum, Figure 3A). Figure 2B displays the ¹³C NMR spectrum in pure H₂SO₄ with added TFA-*d*. The ¹H resonances are found in five groups: an upfield group between 3.5 and 4.1 ppm due to CH–N protons (4H); a multiplet between 2.9 and 3.1 ppm (2H) assigned to the CO–CH protons (2H); a multiplet between 2.5 and 2.7 ppm (2H); a multiplet between 1.8 and 2.0 ppm (3H); and a multiplet between 1.7 and 1.8 ppm (2H). Table 2 lists experimental and calculated (B3LYP/6-31G*) ¹H chemical shifts for **8_{BC}**, calculated chemical shifts for **6_{BC}**, **6_{CC}**, and **7_{BC}**, as well as the experimental chemical shifts of the protonated (i.e., deuterated) lactam (Figure 1B). Although it is the ¹³C NMR spectrum that definitively establishes dominant

Table 2. Comparison between Calculated (B3LYP/6-31G*) and Experimental ^1H NMR Chemical Shifts (CDCl_3) for 8_{BC} , Experimental Chemical Shifts Reported for Approximately Equimolar Amounts of 8_{BC} and H_2SO_4 in $\text{TFA}-d$, and Comparison with Calculated Chemical Shifts for the N-Protonated Conformers 6_{BC} and 6_{CC} and the O-protonated 7_{BC}

proton ^b	8_{BC}		protonated 8_{BC} ^a expt	6_{BC} calcd	6_{CC} calcd	7_{BC} calcd
	expt ^c	calcd				
3H_{fp}	2.47	2.34	2.90–3.10	2.97	3.33 (3H_{eq})	2.70
3H_{eq}	2.34	2.04	2.9–3.1	3.15	3.16 (3H_{ax})	3.13
4H_{ax}	1.40	1.58	1.7–2.0	2.07	2.50	1.85
4H_{eq}	2.26	2.05	2.5–2.7	2.69	2.35	2.84
5H	2.30	1.95	2.5–2.7	2.57	2.30	2.95
6H_{ax}	~1.82	1.74	1.7–2.0	2.03	2.24	2.17
6H_{eq}	~1.51	1.46	1.7–2.0	2.04	2.28	1.83
7H_{ax}	~1.76	1.90	1.7–2.0	2.07	2.24	1.98
7H_{eq}	1.36	0.96	1.7–2.0	2.03	2.25	1.94
8H_{ax}	2.82	2.49	3.51	3.35	3.56	3.70
8H_{eq}	4.12	4.15	4.05	4.09	3.73	3.83
9H_{fp}	3.32	3.23	3.80	3.73	3.79 ($9\text{H}_{\text{ax}}'$)	3.42
9H_{ax}	3.05	2.86	3.61	3.49	3.61	3.49

^a 6_{BC} is demonstrated in this paper to be the major component, with 7_{BC} comprising roughly 20%. ^b For numbering of protons see the Supporting Information, S.1.1. ^c Chemical shifts assigned with the aid of COSY and NOESY. These may be compared with the chemical shifts reported by Brehm et al.^{20h} representing unassigned chemical shift ranges in some cases.

N-protonation (see below), this conclusion is also supported by the ^1H NMR spectrum. O-Protonation is predicted to be characterized by four protons in the range 2.70–3.13 ppm, one proton at 2.17 ppm, and four protons in the range 1.85–1.98 ppm. Both 6_{BC} and 6_{CC} are calculated to have their 3H protons well-separated from the seven remaining higher-field protons, as observed experimentally. The striking similarity (Figure 1) between the four downfield protons (8H_{eq} , 9H_{fp} , 9H_{ax} , 8H_{ax}) in the parent lactam and those in the protonated lactam is fully consistent with structure 6_{BC} . If 6_{CC} were dominant, one would predict additional long-range (W-type) coupling between 9H_{ax} and 4H_{eq} .^{20d} The NOESY spectrum (see the Supporting Information, S.2.13 and S.2.14) indicates proximity of 9H_{fp} and 3H_{fp} (calculated distance 2.368 Å in 6_{BC}) as well as 5H and 4H_{eq} (calculated distance 2.302 Å in 6_{BC}).

Comparison of the ^{13}C NMR spectrum of protonated 8_{BC} (Figure 2B or Figure 3A) with that of the neutral lactam (Figure 2A) is very instructive. Table 3 lists experimental and calculated ^{13}C chemical shifts for 8_{BC} , calculated chemical shifts for 6_{BC} , 6_{CC} , and 7_{BC} , as well as the experimental chemical shifts of the protonated lactam (6_{BC}). Calculations with B3LYP/6-31G* adequately predict the ^{13}C chemical shifts of the carbons in 8_{BC} with the exception of the carbonyl carbon (C2), for which the calculated value is about 14 ppm upfield of the experimental value. This same single discrepancy (ca. 14 ppm upfield) is also seen in comparison of B3LYP/6-31G* and experimental data for N-methyl-2-pyrrolidone (**9**, see Table 4). N-Methyl-2-pyrrolidone, as noted earlier, is calculated to favor O-protonation over N-protonation by 15 kcal/mol. It therefore protonates exclusively on oxygen just as do other unstrained amides.^{6,16} Table 4 also shows the comparison between calculation and experiment for this salt. The calculated chemical shift of the carbonyl carbon of

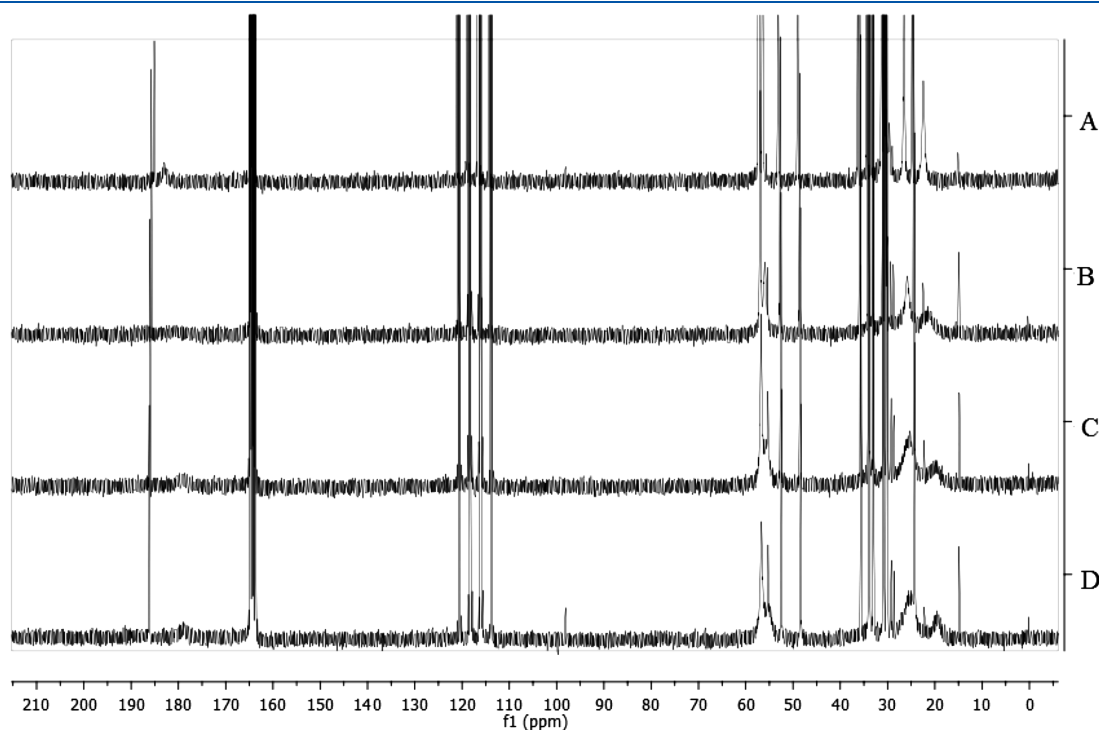


Figure 3. Variable-temperature (25 to $-15\text{ }^\circ\text{C}$) ^{13}C NMR (125 MHz) spectra (A to D, respectively) for 1-azabicyclo[3.3.1]nonan-2-one and roughly equimolar sulfuric acid in $\text{TFA}-d$. There was some hydrolysis of the lactam producing protonated 3-(3-piperidinyl)propionic acid, which supplemented TFA as an internal standard for chemical shift as well as line width.

Table 3. Comparison between Calculated (B3LYP/6-31G*) and Experimental ^{13}C NMR Chemical Shifts (CDCl_3) for 8_{BC} , Experimental Chemical Shifts Reported for Approximately Equimolar Amounts of 8_{BC} and H_2SO_4 in $\text{TFA}-d$, and Comparison with Calculated Chemical Shifts for the N-Protonated Conformers 6_{BC} and 6_{CC} and the O-Protonated 7_{BC}

carbon	8_{BC}		protonated 8_{BC}^a expt ^c	6_{BC} calcd	6_{CC} calcd	7_{BC} calcd
	expt ^b	calcd				
C2	185.0	170.9 ^d	182.5 (v br)	166.8 ^d	163.9 ^d	181.6 ^e
C3	33.4	33.2	34.5	30.4	34.4	31.6
C4	25.0	27.9	25.5 (v sl br)	22.8	28.4	27.9
C5	29.8 ^b	32.2	27.5 (v br)	25.4	26.6	27.3
C6	30.9	32.3	30.5	29.5	26.8	29.6
C7	20.7	21.7	20.5 (sl br)	18.0	20.6	28.5
C8	51.6	51.0	56.5	55.7	53.0	57.0
C9	52.9	52.4	56.0	52.3	56.3	57.7

^a 6_{BC} is demonstrated in this paper to be the major component, with 7_{BC} comprising roughly 20%. ^b These may be compared with the chemical shifts assigned by Brehm et al.^{20h} That study definitively assigned the 29.7 ppm chemical shift to the methine carbon C5. ^c With the exception of C2, the assignments of ^{13}C chemical shifts to specific carbons are approximate, based upon comparison with calculated values, and are discussed further in the text (v br = very broad; sl br = slightly broad; v sl br = very slightly broad). ^d Calculated and experimental results for 8_{BC} and for 2 and 9 (Table 4) suggest that calculated C=O chemical shifts for related species should be corrected by adding 12–14 ppm. This also makes the results for 6_{BC} and 6_{CC} self-consistent. ^e Calculated and experimental results for 1 (Table 4) suggest that calculated C=O chemical shifts for related species should be corrected by adding ca. 10–11 ppm to ca. 192–193 ppm. From a different standpoint, comparison of the calculated chemical shift difference between 6_{BC} and 7_{BC} and the experimental value for 6_{BC} (179 ppm) obtained from the variable-temperature ^{13}C NMR study (see later discussion) suggests ca. 15 ppm correction to 194 ppm. This will be the chemical shift employed in the present study for 7_{BC} .

Table 4. Calculated (B3LYP/6-31G*) and Experimental ^{13}C Chemical Shifts for N-Methyl-2-pyrrolidone (9) and Its O-Protonated Salt (1), As Well As Calculated Values for 1-Azabicyclo[2.2.2]octan-2-one (“ABO”) and Calculated and Experimental Values for Its N-Protonated Salt (2)⁵

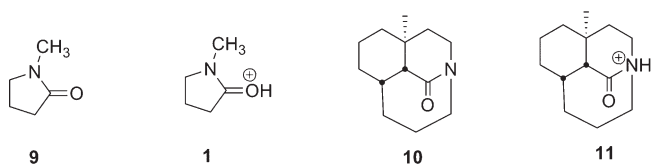
9		1		ABO ^a	2	
expt	calcd	expt	calcd	calcd	expt ⁵	calcd
C2: 174.9	C2: 160.7	C2: 180.5	C2: 169.7	C2: 185.8 ^b	C2: 175.9	C2: 164.0
C3: 30.8	C3: 30.2	C3: 34.7	C3: 32.3	C3: 40.9	C3: 40.1	C3: 39.1
C4: 17.8	C4: 20.6	C4: 19.5	C4: 19.4	C4: 28.8	C4: 25.7	C4: 26.4
C5: 49.1	C5: 47.9	C5: 57.0	C5: 56.0	C5/8: 27.3	C5/8: 22.7	C5/8: 24.3
C6: 29.7	C6: 28.5	C6: 33.1	C6: 33.1	C6/7: 46.1	C6/7: 48.1	C6/7: 48.6

^a ABO = 1-azabicyclo[2.2.2]octan-2-one. ^b Note that the experimental value for 5,6-benzo-1-azabicyclo[2.2.2]octan-2-one is 192.3 ppm,^{4a} whereas the calculated value (B3LYP/6-31G*) is 182.0 ppm. Use of this difference might suggest that the experimental value for ABO should be ca. 196 ppm.

O-protonated N-methyl-2-pyrrolidone (1)²⁵ is ca. 10–11 ppm upfield of the experimental value.

Comparison of Figures 2A and 2B (or Figure 3A) and comparison with Table 3 indicates that upon protonation, the

Scheme 4



carbonyl carbon shift of 8_{BC} moves from 185.0 ppm to higher field (ca. 182.5 ppm). The carbonyl peak in Figure 2B is very broad as is the peak at 27.5 ppm, with those at 20.5 and 25.5 ppm also showing some degree of broadening. The upfield shift is more consistent with the calculated values for 6_{BC} and 6_{CC} after adding ca. 14 ppm (as for 8_{BC}) to the calculated values (see the Discussion below). Similarly, correction of the calculated carbonyl chemical shift for 7_{BC} by adding 10–11 ppm (as for 1, see Table 4) provides a value of about 192–193 ppm, some 7–8 ppm to lower field from the neutral lactams. The prediction of an upfield shift of the carbonyl carbon of a lactam upon protonation at nitrogen appears at first to be counterintuitive. However, there is solid precedent. The annelated [4.3.1] system 10 (Scheme 4), which also has significantly reduced resonance stabilization, has a carbonyl chemical shift of 188.7 ppm.^{7c} The N-protonated salt (11) is more stable than its O-protonated tautomer: Aube demonstrated crystallographic proof of N-protonation using the tetrafluoroborate salt.^{7c} The carbonyl shift in 11 (177.3 ppm) is some 11–12 ppm upfield of that in the neutral lactam.^{7c} In the present study, calculations of 1-azabicyclo[4.3.1]decan-10-one, the core lactam in 10, as well as its N-protonated and O-protonated derivatives, favor N-protonation over O-protonation by 7.9 kcal/mol (comparison between the most stable conformers of each). The calculated ^{13}C chemical shift for the carbonyl carbon in the N-protonated derivative (166.3 ppm) is predicted to be almost 8 ppm upfield of that in the neutral lactam 1-azabicyclo[4.3.1]decan-2-one (174.2 ppm). As already noted, the B3LYP/6-31G* values are about 14 ppm upfield of the experimental values for lactam carbonyl carbons. The calculated difference (8 ppm) is quite comparable to the experimental difference between 10 and 11 (11–12 ppm). An upfield chemical shift of the carbonyl carbon upon N-protonation of a distorted lactam is also seen when one compares the chemical shift reported by Tani and Stoltz^{5a} for 2 (175.9 ppm) with that reported by Somayaji and Brown^{4a} for 5,6-benzo-1-azabicyclo[2.2.2]octan-2-one (192.3 ppm), where both are reported for CD_3CN solutions. Comparison of the calculated value for this last compound (182.0 ppm vs 192.3 ppm experimental) with the calculated value for the presently unknown^{5a} neutral parent compound (185.4 ppm, thus predicting an experimental value of 195.7 ppm for the N-protonated tautomer) suggests that the upfield shift in this system (ca. 20 ppm: 195.7 ppm vs 175.9 ppm) should be even larger than that (11–12 ppm) recorded for 10 and 11. Table 4 includes calculated and experimental chemical shifts for the protonated lactam 2 as well as calculated values for its neutral conjugate base 1-azabicyclo[2.2.2]octan-2-one (“ABO” in Table 4). Further analysis of the carbonyl ^{13}C chemical shift in 6_{BC} versus 8_{BC} will be presented below. Of particular note at present are relative ^{13}C chemical shift values calculated for N-methyl-2-pyrrolidone (9): 160.7 ppm (174.9 ppm, experimental); its O-protonated derivative (1): 169.7 ppm (180.5 ppm experimental); and the N-protonated derivative: 166.2 ppm. For this undistorted lactam, the carbonyl carbon of the

N-protonated derivative is 5–6 ppm *downfield* of the neutral lactam. Similarly, the calculated value for N-protonated *N,N*-dimethylacetamide (162.9 ppm) is 6–7 ppm *downfield* of that in the planar neutral amide (156.0 ppm). Of course, there are no experimental NMR data for the N-protonated salts of these undistorted lactam and amide compounds since they are O-protonated.

On the basis of the ^{13}C chemical shift of the very broad carbonyl carbon peak in protonated 1-azabicyclo[3.3.1]nonan-2-one and comparisons with experimental values for **2** and **1**, as well as computational chemical shifts (corrected), nitrogen is the preferred site of protonation and δ_{BC} and/or δ_{CC} is the major species present in the presence of sulfuric acid. This is certainly consistent with the calculated values in Table 1.

The next question: Is the dominant conformation the boat-chair (δ_{BC}) or chair-chair (δ_{CC})? There are clear similarities in appearance between the four low-field CH–N protons in parts A and B of Figure 1. This suggests the same order in chemical shifts among the CH–N protons just as the calculations predict for δ_{BC} (Table 2). The calculations predict the same order of chemical shifts for the four downfield (CH–N) protons as found experimentally. Furthermore, the calculations for δ_{BC} also reproduce the pattern of two protons in the 2.50–2.70 ppm range and five higher-field protons with very similar chemical shifts. The comparison between calculated versus experimental ^{13}C chemical shifts (Table 3) does not allow a clear choice between δ_{BC} and δ_{CC} . Although the B3LYP/6-31G* and QCISD(T) calculations both predict that δ_{CC} is slightly more stable, the proton NMR data clearly support δ_{BC} as the more stable conformer.

The four broadened ^{13}C resonances shown in Figure 2B suggest the possibility of a dynamic exchange process accessible due to the inherently larger range of ^{13}C chemical shifts. Perhaps there is exchange between protonated and unprotonated lactam? Another possibility is exchange between monoprotonated and diprotonated lactam. However, while diprotonated (but not triprotonated) urea has been experimentally observed in magic acid ($\text{FSO}_3\text{H}\cdot\text{SbF}_5$),²⁶ there are no published observations of an amide or lactam protonated on both heteroatoms of the same linkage. To test these possibilities, 1-azabicyclo[3.3.1]nonan-2-one was dissolved in neat deuterated trifluorosulfonic (triflic) acid (TFSA-*d*). The resulting ^{13}C NMR spectrum (see the Supporting Information, S.2.10) was essentially the same as that obtained with D_2SO_4 and thus only monoprotonated species are present. When “25% Magic Acid” (4:1 $\text{FSO}_3\text{H}/\text{SbF}_5$) was employed as solvent and the ^1H and ^{13}C NMR observed at ambient temperature, it was clear that extensive decomposition of the lactam had occurred (see the Supporting Information, S.2.11 and S.2.12). Another explanation for the broad ^{13}C peaks is exchange among two or all three species (δ_{BC} , δ_{CC} and a lesser amount of δ_{7BC}). The ^{13}C chemical shift differences between potentially exchanging carbons in δ_{BC} and δ_{CC} are relatively small (Table 3). The calculated energy of activation (B3LYP/6-31G*) for inversion of the slightly flattened chair in δ_{BC} to the slightly flattened boat in δ_{CC} is only 1.5 kcal/mol (1.7 kcal/mol aqueous). This exceedingly rapid conformational process cannot be responsible for the broadened peaks in Figure 2B.

To further investigate the source of peak broadening in the ^{13}C NMR spectrum of protonated 1-azabicyclo[3.3.1]nonan-2-one (Figure 2B), a limited variable-temperature study of the carbonyl resonance was conducted at 125 MHz (Figure 3). In this experiment, at ambient temperature it is clear that, for this

run, there has been some hydrolysis of the lactam to the protonated amino acid starting material. This turned out to be fortuitous since the amino acid augmented TFA as a chemical shift internal standard as well as a peak-width standard for nonexchanging resonances. The same 99.98% H_2SO_4 had been used for an extended period by the time this phase of the study was undertaken and had undoubtedly absorbed some moisture from the atmosphere. Since the melting point of TFA is -15°C and the goal of this study was to investigate the origin of the broad peaks rather than a detailed kinetic study, the temperature range investigated was limited (25 to -15°C) and instrument temperature settings rather than precise calibrations were employed.

At 0°C (Figure 3), some very significant changes occurred in the ^{13}C NMR spectrum. Most obvious is that the broad carbonyl resonance (182.5 ppm at 25°C , corresponding to 182.5 ppm in Table 3) has disappeared into the baseline. Also striking is the very marked broadening of the peak at ca. 56 ppm, the higher field of the two sp^3 carbons attached to nitrogen. The other very broad peak (27.5 ppm) has also disappeared into the baseline while the remaining two broad peaks (25.5 and 20.5 ppm) have broadened further. At -10°C , a peak at 179 ppm starts to appear and is more in evidence at -15°C . At -15°C , the resonance at 25.5 ppm appears to be exhibiting coalescence. Our assignments of experimental chemical shifts with calculated chemical shifts are consistent with the broadened peaks corresponding to those with the largest calculated chemical shift differences between δ_{BC} and δ_{7BC} (Table 3).

The changes observed for the carbonyl resonance in Figure 3 are of particular interest. Parts A–D of Figure 4 focus on this peak. The peak at 179 ppm that starts to emerge at -10°C (Figure 4C) and is more apparent at -15°C (Figure 4D) corresponds to the N-protonated tautomer δ_{BC} . For comparison, the corresponding resonances in **2** (~ 176 ppm) and **11** (~ 177 ppm) are very similar to this value (although both **2** and **11** are in acetonitrile solution rather than TFA). The calculated difference between δ_{8BC} and δ_{6BC} (4.1 ppm) is close to the experimental difference (6.0 ppm). This raises the question of the location of the lower-field carbonyl resonance corresponding to the O-protonated tautomer δ_{7BC} . If one simply employs the calculated chemical shift difference between δ_{BC} and δ_{7BC} (see Table 3), the peak for δ_{7BC} should appear around 194 ppm. Using a weighted average of chemical shifts, one calculates an equilibrium mixture of roughly 4:1 ($\delta_{\text{BC}}/\delta_{\text{7BC}}$). This might be a lower limit for this ratio since there is simply no discernible peak in the vicinity of 194 ppm at -15°C . The simulations (Figure 4, parts E–M) indicate that only at very low exchange rate should the minor peak emerge from the background.

Simulation, using Reich's WinDNMR program,²⁷ of the exchange of two singlets in a 4:1 ratio and separated by 15 ppm (179 and 194 ppm) nicely reproduces key features of the experimental data (see Figure 4, parts E–N; the 20% approximation places the time-averaged peak at 182 rather than 182.5 ppm for simplicity's sake). These include the total disappearance of the peak due to its very broad coalescence at 0°C (Figure 4H) and the emergence of the N-protonated lactam peak at 179 ppm with no visible downfield O-protonated peak at 194 ppm at this temperature or as low as -15°C (e.g., Figure 4, parts I–L). The very approximate calculated exchange rates ($k_{\text{ab}} + k_{\text{ba}}$) are as follows: $200\,000\text{ s}^{-1}$ (25°C) (Figure 4G); $12\,000\text{ s}^{-1}$ (0°C) (Figure 4H; this is most uncertain since there is a very wide range of rates ($10\,000$ – $50\,000\text{ s}^{-1}$) corresponding to the disappearance

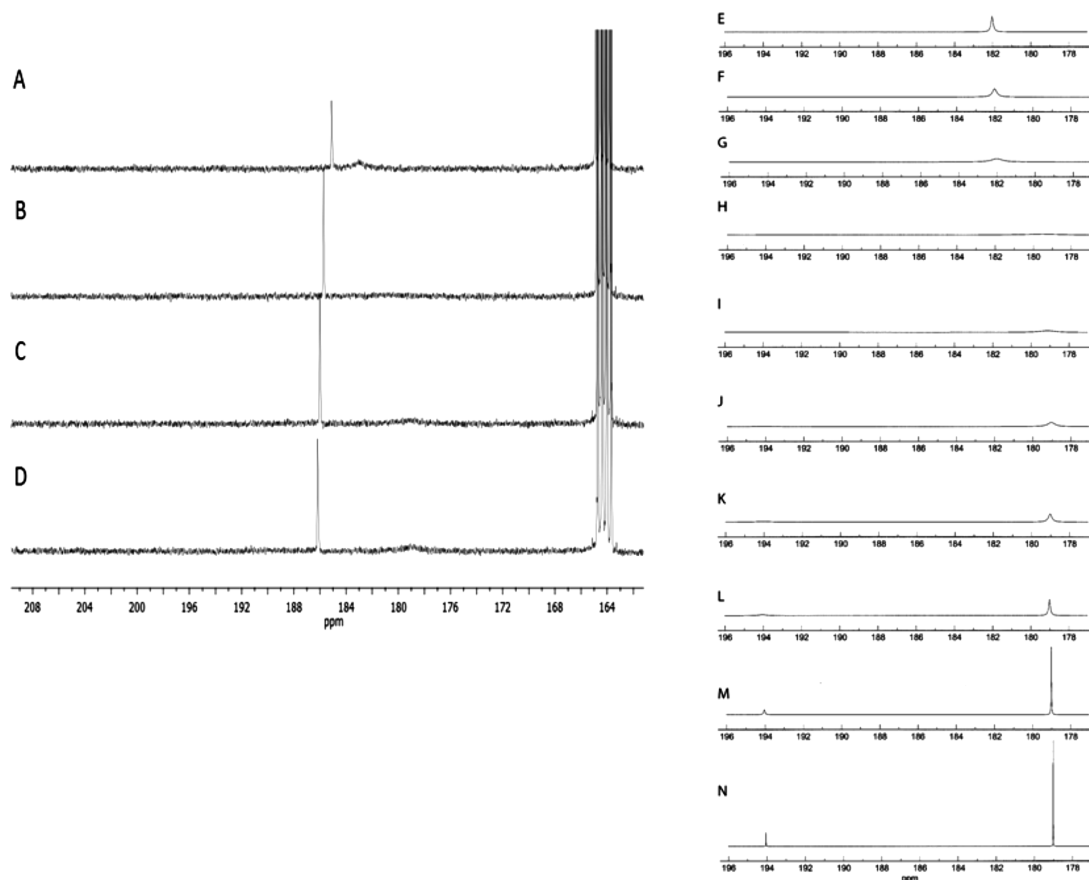


Figure 4. (A–D) Expansion of low-field sections of variable-temperature ^{13}C NMR spectra from Figure 3 from 25 (A) to $-15\text{ }^\circ\text{C}$ (D) respectively. Parts E–N depict simulated WinDNMR²⁷ spectra that correspond to a 4:1 ratio of 6_{BC} and 7_{BC} , having carbonyl carbon chemical shifts of 179 and 194 ppm (estimated), respectively, and calculated exchange rates ($k_{\text{AB}} + k_{\text{BA}}$, s^{-1}) as follows: (E) 1×10^6 ; (F) 5×10^5 ; (G) 2×10^5 ; (H) 1.2×10^4 ; (I) 5×10^3 ; (J) 2×10^3 ; (K) 1×10^3 ; (L) 5×10^2 ; (M) 1×10^2 ; (N) 0.

of peaks at this very broad coalescence); 5000 s^{-1} ($-10\text{ }^\circ\text{C}$) (Figure 4I); and 2000 s^{-1} ($-15\text{ }^\circ\text{C}$) (Figure 4J). The simulated spectra predict that the O-protonated peak at 194 ppm only starts to emerge from baseline at very slow exchange rates (e.g., $<500\text{ s}^{-1}$, see Figure 4L). Figure 4N depicts hypothetical 0 s^{-1} exchange.

The relatively high observed coalescence temperature (ca. $0\text{ }^\circ\text{C}$) is a consequence of the huge chemical shift difference (ca. 15 ppm) estimated for carbonyl carbons in two very different environments. As the simulations (Figure 4E–N) indicate, this chemical shift difference is predicted to yield sharp peaks for the separated carbonyl resonances only at very low exchange rates.

Ultraviolet (UV) spectroscopy is a useful probe for detecting the site of protonation on an amide or lactam. Protonation on nitrogen converts an allylic-type system to an N–H-substituted ketone with the expectation that the $n \rightarrow \pi^*$ absorption will move to longer wavelength, and the $\pi \rightarrow \pi^*$ transition will move to much shorter wavelength.²⁸ Interestingly, UV spectra for unprotonated and protonated derivatives of 2-quinuclidone were reported nearly 50 years ago.^{3c} Since *both* the unprotonated and N-protonated derivatives of 2-quinuclidone are effectively ketones, that study has only partial relevance for the present study. The $n \rightarrow \pi^*$ transition in various methylated 2-quinuclidones is, as predicted,²⁹ found at higher wavelengths (236–247 nm in cyclohexane) than in unstrained lactams or amides (ca. 220 nm).^{3c} The UV spectrum of the N-protonated hydrochloride of the 6,6,7-trimethyl derivative (in water) is reported to include a very broad, indistinct

absorption band (ca. 220–280 nm) and a pronounced blue shift of the $\pi \rightarrow \pi^*$ band. The UV spectrum of the hydrochloride salt of *N,N*-dimethylacetamide (DMA),³⁰ established by X-ray crystallography to be protonated on oxygen, is of considerable interest. In solution, protonation on the DMA oxygen produces a blue shift of ca. 8 nm (200 to 192 nm) in the $\pi \rightarrow \pi^*$ transition.^{3c} This blue shift might in fact be up to 10 nm greater if correction for solvent effects were included.³¹ The DMA hydrochloride is also characterized by weak bands at 315 and 360 nm (CH_2Cl_2 solution), strongly resembling the spectrum observed in aqueous HCl.^{3c} A claim to have observed ca. 0.1% N-protonated DMA²⁸ appears to have been an artifact of solvent effects.³¹

UV spectroscopy is consistent with protonation of 1-azabicyclo[3.3.1]nonan-2-one at nitrogen rather than oxygen. Figure 5A displays the UV spectrum of *N*-methyl-2-pyrrolidone in water. It is dominated by an intense absorbance just below 200 nm due to the $\pi \rightarrow \pi^*$ transition. In good agreement with an earlier study,^{20h} λ_{max} for 1-azabicyclo[3.3.1]nonan-2-one in water occurs at 204 nm (ϵ 7900, Figure 5B) and is associated with the $\pi \rightarrow \pi^*$ transition with a slight shoulder that is likely due to the $n \rightarrow \pi^*$ transition. The UV spectrum of *N*-methyl-2-pyrrolidone in acid solution (Figure 5C) strongly resembles that of protonated DMA, reflecting O-protonation. It includes weak absorptions at ~ 260 and ~ 320 nm and a very slight blue shift of the $\pi \rightarrow \pi^*$ transition in pure sulfuric acid. The UV spectrum of 1-azabicyclo[3.3.1]nonan-2-one in sulfuric acid (Figure 5D) is markedly different from that of protonated

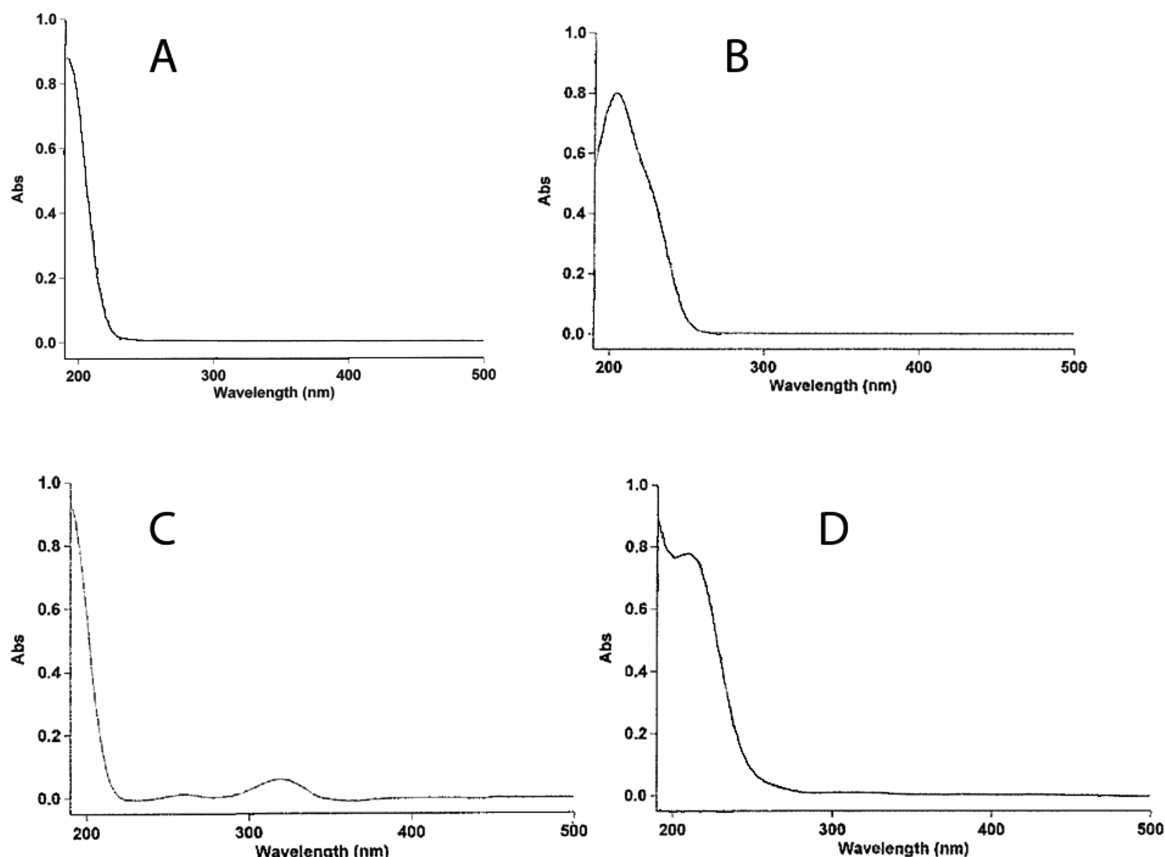


Figure 5. (A) Ultraviolet spectrum of 0.00010 M *N*-methyl-2-pyrrolidone in water; (B) ultraviolet spectrum of 0.00010 M 1-azabicyclo[3.3.1]nonan-2-one in water; (C) ultraviolet spectrum of 0.00010 M *N*-methyl-2-pyrrolidone in pure sulfuric acid; and (D) ultraviolet spectrum of 0.00010 M 1-azabicyclo[3.3.1]nonan-2-one in pure sulfuric acid. The quartz UV cell path length was 1.00 cm.

N-methyl-2-pyrrolidone (Figure 5C). There now appear to be two substantial π - π^* absorbances: the larger one very appreciably blue-shifted and the other very slightly red-shifted to 210 nm. There appears to be a very small trace of an absorbance at ca. 320 nm in Figure 5D.

The significant differences in the UV spectra depicted in parts C and D of Figure 5 are consistent with a dominant change in the site of protonation from oxygen to nitrogen. The features in Figure 5D suggest the possibility of a lesser amount of 7_{BC} in equilibrium with 6_{BC} (although a minor quantity of 6_{CC} would be difficult to distinguish by using UV spectroscopy).

In unstrained amides and lactams, the p-orbital of the planar nitrogen is the major contributor to the HOMO, which resembles ψ_2 of the allylic system, sometimes termed π_N .³² Twisting of the amide is accompanied by pyramidalization of nitrogen^{1b} and transformation of the nitrogen contribution (in π_N) to a lone pair (n_N).³² Comparison of the experimental UV photoelectron spectrum with computational results rationalizes the first two (sharp) bands of the spectrum of 1-azabicyclo[3.3.1]nonan-2-one in terms of n_N as the HOMO and n_O as HOMO-1.³² Our finding that this lactam protonates on nitrogen rather than oxygen is in accord with the predictions of Werstiuk et al.^{8b}

During the investigation of the broadened ¹³C spectra of 6_{BC} the possibility of hydrogen-bonded dimers playing a role in exchange was investigated. Molecular models quickly make it apparent that dimerization of N-protonated chair-chair (6_{CC}) is far better than 6_{BC} . Optimizations (B3LYP/6-31G**/3-21G) of the dimer employing $6_{CB}/6_{CB}$, $6_{CB}/6_{CC}$, and $6_{CC}/6_{CC}$ (each in

Scheme 5



an aqueous continuum) led to $6_{CC}/6_{CC}$ structures as most favorable. Combinations of *R,R* (equivalent to *S,S*) and *R,S* indicated that structure **12** (*R,S*- 6_{CC} , see Scheme 5) has the lowest energy although the energy differences are very small. In aqueous solution the total energy of **12** is 2.1 kcal/mol lower than the separated monomers in aqueous continuum. However, due to losses in translational and rotational entropy as well as the tight organizational order due to two hydrogen bonds, the aqueous monomers are favored by about 10 kcal/mol over the dimer. The calculated ¹³C chemical shifts for **12** (gas phase for comparison purposes) predict a value for C2 of 180.6 ppm in seeming agreement with experiment. However, the caveats in Tables 3 and 4 suggest that this calculated value actually should correspond to an experimental chemical shift of 190–195 ppm. Therefore, there is no evidence supporting the dimer. In principle, 2-quinuclidonium (**2**) can also form an excellent doubly hydrogen-bonded dimer (**13**) as readily as 6_{CC} might. However, this does not appear to be the case⁵ and in the crystal

structure the hydrogen bonding apparent in the crystalline tetrafluoroborate involves $^+N-H\cdots F$.^{5a} Calculations indicate that dimerization of the monomer in aqueous solution also corresponds to a virtually identical favorable change in total energy (-2.1 kcal/mol), but loss of translational and rotational freedom along with the highly ordered structure are factors heavily favoring the monomer. Although a rate of exchange has been estimated for transfer of the proton between nitrogen and oxygen (see above), the kinetics of this process have not been investigated. While it would seem that exchange rates are likely to be pseudo-first order (i.e., proton exchange between the monomer and solvent), the potential formation of dimers (**12**) as intermediates for exchange would be consistent with a process that is second-order in monomer, characterized by a substantial negative entropy of activation.

CONCLUSIONS

1-Azabicyclo[3.3.1]nonan-2-one protonates on nitrogen in agreement with calculations for the gas phase and for aqueous solution. The most obvious support for this conclusion is the upfield chemical shift, relative to the free lactam, of the carbonyl ^{13}C resonance of the protonated species. Calculations predict that the chair-chair conformation of the N-protonated lactam is very slightly more stable than the boat-chair, while the 1H and ^{13}C NMR spectra favor the latter. This is most apparent by comparison of the chemical shifts and coupling patterns of the four downfield protons in **6_{BC}** with those in **8_{BC}**. Conformational exchange between the two conformers is calculated to be exceedingly rapid (energy of activation <2 kcal/mol) and the NMR spectra arise from the dominant conformer (**6_{BC}**) with little if any broadening due to the similarities in the 1H and ^{13}C NMR chemical shifts of the two conformers. There is, however, an exchange process apparent through variable-temperature ^{13}C NMR spectroscopy, even at ambient temperature. It corresponds to dynamic exchange between the dominant N-protonated tautomer and the minor (ca. 20%) O-protonated tautomer. The large chemical shift difference between the carbonyl carbons of **6_{BC}** and **7_{BC}** (ca. 15 ppm calculated) contributes to making this exchange observable at moderately low temperatures.

The UV spectrum of *N*-methyl-2-pyrrolidone in sulfuric acid bears strong resemblance to the UV spectrum of the hydrochloride salt of *N,N*-dimethylacetamide, established by X-ray crystallography to be O-protonated. The UV spectrum of 1-azabicyclo[3.3.1]nonan-2-one in sulfuric acid shows marked differences compared to the corresponding spectrum for *N*-methyl-2-pyrrolidone. Its UV spectrum is compatible with the simultaneous presence of N-protonated and O-protonated tautomers with the former being the major species. Taken together with the simulated ^{13}C dynamic NMR study and the predictions of the calculations, this appears to be the first observation of an amide or lactam with measurable quantities of N-protonated and O-protonated species in equilibrium. The results also support the finding of Werstiuk et al. that the nature of the HOMO (n_O or n_N) of a twisted bridgehead lactam determines the site of protonation (oxygen or nitrogen).

The doubly hydrogen-bridged dimer of chair-chair N-protonated 1-azabicyclo[3.3.1]nonan-2-one has an attractive structure and, in aqueous solution, has a calculated total energy over 2 kcal/mol lower than the separated monomeric cations. However, the free energy of the dimer is considerably higher than that of the two monomers and there is no evidence for the dimer in

solution. 2-Quinuclidonium can, in principle, form an analogous dimer and the energy considerations are almost identical with those of the aforementioned [3.3.1] system. However, the Tani and Stoltz study showed no evidence of the dimer in solution. In the solid state, there is hydrogen bonding between 2-quinuclidonium and its counterion BF_4^- . Although proton exchange is likely to occur between the monomer and solvent, it is conceivable that dimerization may furnish a viable, but entropically demanding, pathway for simultaneous exchange of two N-protons with two O-protons. Detailed investigation of the mechanism of the tautomerism between **6_{BC}** and **7_{BC}** is a project for future study.

Since pyramidalization at the carbonyl carbon (χ_C) in distorted lactams and amides is usually quite small, this allows the distortion energy surface to be three-dimensional. The present case provides one experimental point on such a surface ($\tau = 20^\circ$; $\chi_N = 50^\circ$) where N-protonation and O-protonation are almost equienergetic. Complexing species other than protons should exhibit markedly different distortion energy surfaces. "Hard" Lewis acids such as Na^+ should intrinsically favor oxygen complexation and require greater pyramidalization and twisting to complex nitrogen; "softer" Lewis acids such as Cu^{2+} should require little distortion in order to complex to the amide nitrogen.^{2c} This is consistent with the function of Cu^{2+} discovered by Eakin et al. in reducing the activation barrier to *cis-trans* peptidyl-prolyl isomerization of β -2-microglobulin.^{14g} This is also an area for future study.

EXPERIMENTAL SECTION

NMR Spectra. 1H and ^{13}C NMR spectra were run at 400 and 100.5 MHz, respectively, on a Varian Mercury spectrometer. The variable-temperature ^{13}C NMR spectra were run at 125.7 MHz on a Varian Inova 500 MHz spectrometer. Spectra were referenced (ppm) against TMS except in the experiments involving protonation with sulfuric acid, where trifluoroacetic acid-*d* (TFA-*d*) (^{13}C and residual 1H) served as internal standard as well as the ^{13}C spectrum in triflic acid (CF_3SO_3H) where the solvent also served as internal standard.

UV Spectra. Ultraviolet spectra were obtained with a Cary 50 Bio (Varian) spectrometer with 1.00 cm thickness quartz cells and the resulting spectra were analyzed with Cary WinUV version 3.00(182) software. For 1-azabicyclo[3.3.1]nonan-2-one, 0.0014 g was dissolved in 10.0 mL of solvent (water or 99.98% sulfuric acid) and diluted 1:10 in the same solvent to produce a 0.00010 M solution. Similarly, 0.0010 g of *N*-methyl-2-pyrrolidone was dissolved in 10.0 mL of solvent and diluted 1:10 to produce a 0.00010 M solution.

Synthetic Procedures

3-(3-Piperidyl)propionic Acid Hydrochloride: In a slight modification of published procedure,^{20a,b} *trans*-3-(3-pyridyl)acrylic acid (11.2 g, 0.080 mol) in 100 mL of glacial acetic acid was hydrogenated over 0.75 g of 10% Pd on charcoal in a stainless steel bomb with stirring (Pressure Products Industries, Inc.) over the course of 6 days maintaining a maximum hydrogen pressure of 600 psi during this period.^{20a,b} The resulting solution was filtered through Celite three times and the filtrate concentrated to a brown syrup on a steam bath/rotovaporator. The resulting oil was dissolved in absolute ethanol (1:15 mol ratio) and 6.0 M hydrochloric acid was added until precipitation was complete. The white precipitate was filtered; the yield of hydrochloride was 8.0 g (70.7% yield overall): mp 219–220 °C; 1H NMR (400 MHz, $DMSO-d_6$) δ 1.12 (m, 1H), 1.45 (m, 2H), 1.67 (m, 4H), 2.24 (t, 2H), 2.50 (broad q, 1H), 2.70 (broad q, 1H), 3.15 (broad d, 2H), 8.89 (broad s, 1H), 9.23 (broad s, 1H), 12.15 (s, 1H); ^{13}C NMR (100.5 MHz, $DMSO-d_6$) δ 22.3, 28.5, 28.8, 31.3, 33.0, 43.8, 48.2, 174.9; ^{13}C NMR (100.5 MHz, TFA-*d*) δ 24.2, 29.6, 30.1, 33.0, 35.7, 48.6, 52.7, 189.5.

1-Azabicyclo[3.3.1]nonan-2-one.^{20h}. A 354 mg (1.85 mmol) sample of 3-(3-piperidyl)propionic acid hydrochloride and 665 mg (2.67 mmol) of di-*n*-butyltin(IV) oxide in 1200 mL of toluene is refluxed with a Dean–Stark trap for 16 h. The solution is concentrated to a yellow oil with use of rotoevaporation. Flash chromatography on silica gel with ethanol:hexanes (4:1) furnished the product (mp 79–81 °C for racemate; lit. values 77–79 °C^{20c} and 77–81 °C^{20g}). ¹H NMR (400 MHz, CDCl₃) δ 1.36 (m, 1H), 1.40 (ddd, 1H), 1.51 (broad d, 1H), 1.76–1.82 (m, 2H), 2.26–2.34 (m, 3H), 2.47 (ddd, 1H), 2.82 (ddd, 1H), 3.05 (d, 1H), 3.32 (dd, 1H), 4.12 (ddd, 1H); ¹³C NMR (100.5 MHz, CDCl₃) δ 20.7, 25.0, 29.8, 30.9, 33.4, 51.6, 52.9, 185.0. [The NMR spectra include minor contributions from pump oil: ¹H NMR (m, 0.83–0.89 ppm; 1.26 ppm); ¹³C NMR (29.8 ppm).]

Protonated 1-Azabicyclo[3.3.1]nonan-2-one: 1-Azabicyclo[3.3.1]nonan-2-one was initially protonated in 99.98% H₂SO₄ or D₂SO₄ with CF₃CO₂D (TFA-*d*) as an internal standard. Subsequent studies were performed with H₂SO₄ approximately equimolar to the lactam in TFA-*d* as solvent (see the Supporting Information). ¹H NMR (400 Hz, TFA-*d*) δ 1.70–2.00 (m, 5H), 2.50–2.70 (m, 2H), 2.90–3.10 (m, 2H), 3.51 (ddd, 1H), 3.61 (d, 1H), 3.80 (broadened d, 1H), 4.05 (broadened d, 1H); ¹³C NMR (100.5 MHz, TFA-*d*) δ 20.5, 25.5, 27.5, 30.5, 34.5, 56.0, 56.5, 182.5. Studies were also performed in triflic acid (CF₃SO₃H) as well as in 25% Magic Acid (i.e., 4:1 fluorosulfuric acid/antimony pentafluoride).

Protonated *N*-Methyl-2-pyrrolidone: The lactam was dissolved in 99.98% H₂SO₄ with TFA-*d* added as internal standard. ¹³C NMR (TFA-*d*, ppm) δ 19.5, 33.1, 34.7, 57.0, 180.5. This may be compared with the results for the neutral lactam: ¹³C NMR (CDCl₃) δ 16.8, 28.6, 29.8, 48.5, 173.9 (see the Supporting Information for these spectra).

■ ASSOCIATED CONTENT

Supporting Information. Experimental procedures, ¹H and ¹³C NMR spectra, total energies, full geometries, zero point energies, and thermal corrections for all structures. This material is available free of charge via the Internet at <http://pubs.acs.org>.

■ AUTHOR INFORMATION

Corresponding Author

*E-mail: art.greenberg@unh.edu.

■ ACKNOWLEDGMENT

The authors wish to thank Professors Richard Johnson, Glen Miller, and Sterling Tomellini, Dr. Patricia Stone Wilkinson, and Ilia Terova for helpful discussions and suggestions.

■ REFERENCES

- (1) (a) Dunitz, J. D.; Winkler, F. K. *Acta Crystallogr., Sect. B* **1975**, *31*, 251–263. (b) Wiberg, K. B. In Greenberg, A.; Breneman, C. M.; Liebman, J. F. In *The Amide Linkage: Structural Significance in Chemistry, Biochemistry, and Materials Science*; John Wiley & Sons: New York, 2000; pp 33–45. (c) Yamada, S. J. In Greenberg, A.; Breneman, C. M.; Liebman, J. F. *The Amide Linkage: Structural Significance in Chemistry, Biochemistry, and Materials Science*; John Wiley & Sons: New York, 2000; pp 215–246.
- (2) (a) Hall, H. K., Jr.; El-Shekeil, A. *Chem. Rev.* **1983**, *83*, 549–555. (b) Greenberg, A. In Liebman, J. F.; Greenberg, A. *Structure and Reactivity*; VCH Publishers Inc.: New York, 1988; pp 139–178. (c) Greenberg, A. In Greenberg, A.; Breneman, C. M.; Liebman, J. F. *The Amide Linkage: Structural Significance in Chemistry, Biochemistry, and Materials Science*; John Wiley & Sons: New York, 2000; pp 47–83. (d)

Mucsi, Z.; Tsai, A.; Szori, M.; Chass, G. A.; Viskolcz, B.; Czismadia, I. G. *J. Phys. Chem. A* **2007**, *111*, 13245–13254.

(3) (a) Pracejus, H. *Chem. Ber.* **1959**, *92*, 988. (b) Pracejus, H. *Chem. Ber.* **1965**, *98*, 2897. (c) Pracejus, H.; Kehlen, M.; Kehlen, H.; Matschiner, H. *Tetrahedron* **1965**, *21*, 2257–2270. (d) Blackburn, G. M.; Skaife, C. J.; Kay, I. T. *J. Chem. Res., Miniprint* **1980**, 3650–3668. Greenberg, A.; Wu, G.; Tsai, J. C.; Chin, Y. Y. *Struct. Chem.* **1993**, *4*, 127–129.

(4) (a) Somayaji, V.; Brown, R. S. *J. Org. Chem.* **1986**, *51*, 2676–2686. (b) Somayaji, V.; Skorey, K. I.; Brown, R. S.; Ball, R. G. *J. Org. Chem.* **1986**, *51*, 4866–4872. (c) Bennet, A. J.; Wang, Q. P.; Slebocka-Tilk, H.; Somayaji, V.; Brown, R. S. *J. Am. Chem. Soc.* **1990**, *112*, 6383–6385. (d) Wang, Q. P.; Bennet, A. J.; Brown, R. S.; Santarsiero, B. D. *J. Am. Chem. Soc.* **1991**, *113*, 5757–5765. (e) Bennet, A. J.; Somayaji, V.; Brown, R. S.; Santarsiero, B. D. *J. Am. Chem. Soc.* **1991**, *113*, 7563–7571. (f) Brown, R. S. In Greenberg, A.; Breneman, C. M.; Liebman, J. F. *The Amide Linkage: Structural Significance in Chemistry, Biochemistry and Material Science*; John Wiley & Sons: New York, 2000; pp 85–114.

(5) (a) Tani, K.; Stoltz, B. M. *Nature* **2006**, *441*, 731–734. (b) Ly, T.; Krout, M.; Pham, D. K.; Tani, K.; Stoltz, B. M.; Julian, R. R. *J. Am. Chem. Soc.* **2007**, *129*, 1864–1865.

(6) (a) Greenberg, A.; Venanzi, C. A. *J. Am. Chem. Soc.* **1993**, *115*, 6951–6957. (b) Greenberg, A.; Moore, D. T.; DuBois, T. D. *J. Am. Chem. Soc.* **1996**, *118*, 8658–8668.

(7) (a) Szostak, M.; Yao, L.; Aube, J. *J. Org. Chem.* **2009**, *74*, 1869–1875. (b) Szostak, M.; Yao, L.; Aube, J. *J. Am. Chem. Soc.* **2010**, *132*, 2078–2084. (c) Szostak, M.; Yao, L.; Day, V. W.; Powell, D. R.; Aube, J. *J. Am. Chem. Soc.* **2010**, *132*, 8836–8837.

(8) (a) Werstiuk, N. H.; Brown, R. S.; Wang, Q. *Can. J. Chem.* **1996**, *74*, 524–532. (b) Werstiuk, N. H.; Muchall, H. M.; Roy, C. D.; Ma, J.; Brown, R. S. *Can. J. Chem.* **1998**, *76*, 672–677.

(9) (a) Kirby, A. J.; Komarov, I. V.; Wothers, P. D.; Feeder, N. *Angew. Chem., Int. Ed.* **1998**, *37*, 785–786. (b) Kirby, A. J.; Komarov, I. V.; Feeder, N. *J. Am. Chem. Soc.* **1998**, *120*, 7101–7102. (c) Kirby, A. J.; Komarov, I. V.; Kowski, K.; Rademacher, P. *J. Chem. Soc., Perkin Trans. 2* **1999**, 1313–1316.

(10) Morgan, K. M.; Rawlins, M. L.; Montgomery, M. N. *J. Phys. Org. Chem.* **2005**, *18*, 310–314.

(11) Lei, Y.; Wroblewski, A. D.; Golden, J. E.; Powell, D. R.; Aube, J. *J. Am. Chem. Soc.* **2005**, *127*, 4552–4553.

(12) Boyd, D. B. In Greenberg, A.; Breneman, C. M.; Liebman, J. F. *The Amide Linkage: Structural Significance in Chemistry, Biochemistry, and Materials Science*; John Wiley & Sons: New York, 2000; pp 337–375.

(13) Mujika, J. I.; Formoso, E.; Mercero, J. M.; Lopez, X. *J. Phys. Chem. B* **2006**, *110*, 15000–15011.

(14) (a) Harrison, R. K.; Stein, R. L. *Biochemistry* **1990**, *29*, 1684–1689. (b) Liu, J.; Albers, M. W.; Chen, C. M.; Schreiber, S. L.; Walsh, C. T. *Proc. Natl. Acad. Sci. U.S.A.* **1990**, *87*, 2304–2308. (c) Fischer, G. *Chem. Soc. Rev.* **2000**, *29*, 119–127. (d) Cox, C.; Leckta, T. *Acc. Chem. Res.* **2000**, *33*, 849–858. (e) Wedemeyer, W. J.; Welker, E.; Scheraga, H. A. *Biochemistry* **2002**, *41*, 14637–14644. (f) Bhat, R.; Wedemeyer, W. J.; Scheraga, H. A. *Biochemistry* **2003**, *42*, 5722–5728. (g) Eakin, C. M.; Berman, A. J.; Miranker, A. D. *Nat. Struct. Mol. Biol.* **2006**, *13*, 202–208.

(15) Johansson, D. G. A.; Wallin, G.; Sandberg, A.; Macao, B.; Åqvist, J.; Härd, T. *J. Am. Chem. Soc.* **2009**, *131*, 9475–9477.

(16) (a) Birchall, T.; Gillespie, R. *J. Am. Chem. Soc.* **1963**, *41*, 2642–2649. (b) Olah, G. A.; White, A. M. *Chem. Rev.* **1970**, *70*, 561–591. Klumpp, D. A.; Rendy, R.; Zhang, Y.; Gomez, A.; McElrea, A. *Org. Lett.* **2004**, *6*, 1789–1792.

(17) (a) Mujika, J. I.; Mercero, J. M.; Lopez, X. *J. Phys. Chem. A* **2003**, *107*, 6099–6107. (b) Mujika, J. I.; Mercero, J. M.; Lopez, X. *J. Am. Chem. Soc.* **2005**, *127*, 4445–4453.

(18) *Spartan 08*, 1.2.0, Wavefunction, Inc., Irvine, CA, 2008.

(19) Frisch, M. J.; Trucks, G. W.; Schlegel, H. B.; Scuseria, G. E.; Robb, M. A.; Cheeseman, J. R.; Montgomery, J. A., Jr.; Vreven, T.; Kudin, K. N.; Burant, J. C.; Millam, J. M.; Iyengar, S. S.; Tomasi, J.; Barone, V.; Mennucci, B.; Cossi, M.; Scalmani, G.; Rega, N.; Petersson,

G. A.; Nakatsuji, H.; Hada, M.; Ehara, M.; Toyota, K.; Fukuda, R.; Hasegawa, J.; Ishida, M.; Nakajima, T.; Honda, Y.; Kitao, O.; Nakai, H.; Klene, M.; Li, X.; Knox, J. E.; Hratchian, H. P.; Cross, J. B.; Bakken, V.; Adamo, C.; Jaramillo, J.; Gomperts, R.; Stratmann, R. E.; Yazyev, O.; Austin, A. J.; Cammi, R.; Pomelli, C.; Ochterski, J. W.; Ayala, P. Y.; Morokuma, K.; Voth, G. A.; Salvador, P.; Dannenberg, J. J.; Zakrzewski, V. G.; Dapprich, S.; Daniels, A. D.; Strain, M. C.; Farkas, O.; Malick, D. K.; Rabuck, A. D.; Raghavachari, K.; Foresman, J. B.; Ortiz, J. V.; Cui, Q.; Baboul, A. G.; Clifford, S.; Cioslowski, J.; Stefanov, B. B.; Liu, G.; Liashenko, A.; Piskorz, P.; Komaromi, I.; Martin, R. L.; Fox, D. J.; Keith, T. M.; Al-Laham, M. A.; Peng, C. Y.; Nanayakkara, A.; Challacombe, M.; Gill, P. M. W.; Johnson, B.; Chen, W.; Wong, M. W.; Gonzalez, C.; Pople, J. A. *Gaussian 03*, Revision E.01; Gaussian Inc., Wallingford, CT, 2004.

(20) (a) Shaw, R. G., Jr. 1-Azabicyclo[3.3.1]nonan-2-one: A Two Chair Bicyclic Lactam Containing Bridgehead Nitrogen, Masters Degree Thesis, The University of Arizona, 1979 [Note: the initial assignment of the double-chair conformation was due to an error in assigning the chemical shifts (at 60 MHz) of the two anisochronous ^9H protons. The authors adopted the boat-chair conformation shortly afterward: see ref 17b]; (b) Hall, H. K., Jr. *J. Am. Chem. Soc.* **1960**, *82*, 1209–1215. (c) Hall, H. K., Jr.; Shaw, R. G., Jr.; Deutschmann, A. *J. Org. Chem.* **1980**, *45*, 3722–3724. (d) Buchanan, G. L. *J. Chem. Soc., Chem. Commun.* **1981**, 814–815. (e) Buchanan, G. L.; Kitson, D. H.; Mallinson, P. R.; Sim, G. A.; White, D. N. J.; Cox, P. J. *J. Chem. Soc., Perkin Trans. 2* **1983**, 1709–1712. (f) Buchanan, G. L. *J. Chem. Soc., Perkin Trans. 1* **1984**, 2669–2670. (g) Steliou, K.; Poupart, M. A. *J. Am. Chem. Soc.* **1983**, *105*, 7130–7138. (h) Brehm, R.; Ohnhäuser, D.; Gerlach, H. *Helv. Chim. Acta* **1987**, *70*, 1981–1987.

(21) Lide, D. A., Ed.-in-Chief *CRC Handbook of Chemistry and Physics*, 90th ed.; CRC Press: Boca Raton, FL, 2009–2010; pp 8–42.

(22) Cox, R. A.; Druet, L. M.; Klausner, A. E.; Modro, T. A.; Wan, P.; Yates, P. *Can. J. Chem.* **1981**, *59*, 1568–1573.

(23) National Institute of Standards and Technology, *NIST Chemistry WebBook*, <http://webbook.nist.gov/chemistry/>. Accessed on January 1, 2011.

(24) Typical Values of ^{13}C NMR chemical shifts for trifluoroacetic acid (Spectral Data Services, NMR Solvent Chemical Shifts Table; www.sdsnmr.com/cs_table.html; accessed on December 15, 2010).

(25) An interesting point is that while protonation of *N*-methylpyrrolidone in solution and in the gas phase is widely understood to occur on oxygen, fragmentation of this ion in electrospray/mass spectrometry is consistent with tautomerization to the *N*-protonated ion prior to fragmentation. Crotti, A. M.; Fonseca, T.; Hong, H.; Staunton, J.; Galembeck, S. E.; Lopes, N. P.; Gates, P. J. *Int. J. Mass Spectrom.* **2004**, *232*, 271–276. This may make the interpretation of the site of protonation in the gas phase more difficult. In this regard the collision-induced dissociation experiments of Ly et al.^{5b} may also be of interest.

(26) Rasul, G.; Prakash, G. K. S.; Olah, G. A. *J. Org. Chem.* **1994**, *59*, 2552–2556.

(27) Reich, H. J. WinDNMR: Dynamic NMR Spectra for Windows *J. Chem. Educ., Software 3D2*.

(28) Benderly, H.; Rosenheck, K. *J. Chem. Soc., Chem. Commun.* **1972**, 179–180.

(29) Bednářová, L.; Maloň, P.; Bouř, P. *Chirality* **2007**, *19*, 775–786.

(30) Benedetti, E.; Di Blasio, B. *J. Chem. Soc., Perkin II* **1980**, 500–503.

(31) Cox, R. A.; Yates, K. *Can. J. Chem.* **1981**, *59*, 1560–1567.

(32) (a) Treschanke, L.; Rademacher, P. *THEOCHEM* **1985**, *122*, 35–45. (b) Treschanke, L.; Rademacher, P. *THEOCHEM* **1985**, *122*, 47–56. (c) Rademacher, P. In Greenberg, A.; Breneman, C. M.; Liebman, J. F. *The Amide Linkage: Structural Significance in Chemistry, Biochemistry, and Materials Science*; John Wiley & Sons: New York, 2000; pp 247–289.